Conduction mechanism in Polyaniline-flyash composite material for shielding against electromagnetic radiation in X-band & Ku band

Avanish Pratap Singh, Anoop Kumar S., Amita Chandra, and S. K. Dhawan

Citation: AIP Advances **1**, 022147 (2011); doi: 10.1063/1.3608052
View online: http://dx.doi.org/10.1063/1.3608052
View Table of Contents: http://aipadvances.aip.org/resource/1/AAIDBI/v1/i2
Published by the American Institute of Physics.

Conduction mechanism in Polyaniline-flyash composite material for shielding against electromagnetic radiation in X-band & Ku band

Avanish Pratap Singh,[1,2] Anoop Kumar S.,[1] Amita Chandra,[2] and S. K. Dhawan[1,a]

[1]*Polymeric & Soft Materials Section, National Physical Laboratory (CSIR), New Delhi – 110 012, India*

[2]*Department of Physics & Astrophysics, University of Delhi, Delhi – 110 007, India*

(Received 31 March 2011; accepted 3 June 2011; published online 23 June 2011)

β–Naphthalene sulphonic acid (β–NSA) doped polyaniline (PANI)–flyash (FA) composites have been prepared by chemical oxidative polymerization route whose conductivity lies in the range 2.37–21.49 S/cm. The temperature dependence of electrical conductivity has also been recorded which shows that composites follow Mott's 3D–VRH model. SEM images demonstrate that β–NSA leads to the formation of the tubular structure with incorporated flyash phase. TGA studies show the improvement in thermal stability of composites with increase in loading level of flyash. Complex parameters i.e. permittivity ($\varepsilon^* = \varepsilon' - i\varepsilon''$) and permeability ($\mu^* = \mu' - i\mu''$) of PANI-FA composites have been calculated from experimental scattering parameters (S_{11} & S_{21}) using theoretical calculations given in Nicholson–Ross and Weir algorithms. The microwave absorption properties of the composites have been studied in X-band (8.2 – 12.4 GHz) & Ku–Band (12.4 – 18 GHz) frequency range. The maximum shielding effectiveness observed was 32dB, which strongly depends on dielectric loss and volume fraction of flyash in PANI matrix. [doi:10.1063/1.3608052]

I. INTRODUCTION

In recent times, the development of electrical and electronic devices has lead to a new type of pollution commonly referred to as electromagnetic interference (EMI). This is a serious concern and affects the life time, efficiency and the safety operation of many electronic devices. In order to avoid such problems, all electronic equipments must be shielded against electromagnetic aggressions. Generally metal, metal oxides and magnetic materials are used for this purpose which has certain limitations. Inherently, conducting polymers (IPCs) along with their wide spread applications in organic light emitting diodes (OLED)[1] polymer solar cells,[2] antistatic coatings[3] and electro chromic devices[4] are also finding their application as shielding materials for electromagnetic radiation.[5] Composites based on polymers like hexagonal–ferrite/polymer, metal/polymer composites and single wall carbon nano tube–epoxy composites[5,6] have been reported by many research groups for this purpose. Conducting polymer composites/blends of polyaniline, polypyrrole and polyethylene dioxythiophene with different dielectrics TiO_2, flyash and ferrites like γ–Fe_2O_3, Fe_3O_4, of Fe-Ni ferrites have been prepared by different methods.[7–9] These composites of conducting polymer have prolonged their sphere and currently finding their application EMI shielding technology.[10]

There is growing concern with respect to topics related to the environment. Coal–burning thermal power plants produce large amounts of flyash (FA) as a residue. In order to minimize these residues, FA has been used in construction, agriculture, metal recovery, water and atmospheric

[a]E-mail: skdhawan@mail.nplindia.ernet.in Fax No. 91-11-25726938

pollution control.[11] There have been many experiments on FA for technical studies and possible applications. Electrically insulating nature of FA, makes it desirable to regulate conductivity of polymer composite.[8,9] In the present study, waste FA has been incorporated in polyaniline by insitu polymerization. The addition of FA results in an enhancement of microwave absorption with an added advantage of industrial waste utilization. The paper reports the electrical and microwave absorption properties of polyaniline–flyash (PF) composites prepared by insitu emulsion polymerization of aniline with FA in the presence of β–NSA. The different compositions have been prepared by taking different concentrations of FA in PANI. From the observed results, it has been concluded that PANI–FA composites have better EMI shielding properties, reduction of skin depth and radiation scattering by FA constituents. The shielding effectiveness value upto 32dB (PF13) has been achieved, which strongly depends on dielectric loss and volume fraction of FA in polyaniline matrix.

II. EXPERIMENTAL SECTION

A. Materials

Aniline (Loba Chemie, India), β–naphthalene–2–sulfonic acid (β–NSA, Himedia, India) and ammonium persulfate (APS, Merck, India) has been used in present study. The aniline monomer has been purified by distillation under reduced presser before use. The other chemicals used are of reagent grade and used as received. Aqueous solutions have been prepared using double distilled water having specific resistivity of 10^6 Ωcm.

B. Synthesis of polyaniline–flyash (PANI-FA) composites

The chemical oxidative polymerization of aniline to prepare PANI–FA composites has been carried out in the presence of FA particles and β–NSA as the dopant without an external template. This method belongs to the self assembly process[12] because β–NSA work as dopant and template functioning at the same time. A typical preparation process for PANI–FA composite is as follows: 0.3 M solution of β–NSA and calculated amount of FA has been homogenized for 2 hrs to obtain a uniform suspension containing FA particles. To this, 0.1 M aniline has been added and stirring continued for another 1h to form an emulsion. The aniline–β–NSA mixture containing FA particles has been cooled in an ice bath for 2 hrs before oxidative polymerization. Finally the oxidant APS (0.1 M) has been added drop wise to the above solution keeping the temperature of the reactor at 0°C with vigorous stirring for 9–10 hrs. The green polymer precipitates so obtained have been treated with methanol. The resulting precipitate has then been filtered and washed thoroughly till the filtrate became colorless and then dried at 60–65°C in a vacuum oven for 24 hrs. Throughout the experiment, the molar ratio of aniline to β–NSA and APS has been retained at 1:3 and 1.0 respectively. But the concentration of FA particles has been changed to understand the effect of FA particles on the morphology, structure, electrical properties and shielding effectiveness of the resulting PANI–FA composite tubes. Several compositions having different AN: FA weight ratios i.e. 1:0, 1:1, 1:2 and 1:3, have been prepared and designated as PF10, PF11, PF12 and PF13 respectively.

C. Characterization

The morphology of PANI–β–NSA tubes and its composites have been examined using scanning electron microscope (SEM, Zeiss EVO MA–10). The SEM samples have been prepared by dispersing the powder in iso–propanol using sonification and placing small drops of the suspension on silicon wafers and sputter–coated with gold before analysis. The semi crystalline nature of PANI–β–NSA and PANI-FA composite has been confirmed by X–ray diffraction (XRD) studies[13] carried out on D8 Advance X–ray diffractometer (Bruker) using CuKα radiation (λ= 1.540598Å) in the scattering range (2θ) of 20°–80° with a scan rate of 0.02°/sec and slit width of 0.1mm. The electrical conductivity of PANI-FA composites have been measured by a standard four–probe technique using Keithley programmable current source (Model 6221) and nanovoltmeter (Model 2182A) attached to a digital temperature controller (Lakeshore 331) and a cryocooler from 285–70K. For electrical

conductivity measurements, rectangular pellets (13x7mm^2) have been prepared from powder sample using rectangular die and hydraulic press at compression pressure of 5 ton. Four ohmic contacts have been made on each end of pellet using silver epoxy paste. Thermogravimetric analyzer (Mettler Toledo TGA/SDTA 851^e) has been used to measure the thermal stability[13] of the material under inert atmosphere (flowing N_2 gas) in the temperature range 25–800°C. The samples have also been studied by UV–visible (Shimadzu UV–1601) spectrophotometer.[13] Electromagnetic shielding and dielectric measurements have been carried out using Agilent E8362B Vector Network Analyzer in the 8.2 – 12.4 GHz (X-band) and 12.4–18GHz (Ku–band) microwave range. Powder samples have been compressed in the form of rectangular pellets (∼2mm thick) and inserted in copper sample holder connected between the wave–guide flanges of network analyzer.

III. RESULTS AND DISCUSSION

The PANI–FA composites have been prepared by in–situ emulsion polymerization using AN–FA as dispersed phase and water as continuous phase. Due to its amphiphilic nature, β–NSA molecule (with hydrophilic SO_3H head and hydrophobic tail) possesses surfactant characteristics and easily forms micelles in aqueous solution. As mentioned in the experiment, FA particles were dispersed in β–NSA aqueous solution before polymerization. As a result, micelles containing FA particles form in the reaction. These micelles have core–shell structure where FA particles are allocate as a core of the micelles due to their hydrophobic nature while β–NSA is regarded as the "shell" due to its hydrophilic group $–SO_3H$. Further, aniline reacts with β–NSA to form an aniline/β–NSA salt via an acid/base reaction. The aniline/β–NSA micelles act as a soft template with the formation of oil in water type emulsion. Thus, the formed anilinium cations might be absorbed on the plane of those core-shell micelles to form spherical micelles by aggregation. At the same time, free aniline existing in the reaction solution might diffuse into those micelles to form aniline-filled micelles. Thus, those micelles containing FA with or without free aniline act as templates in the formation tube like structure of polymer composite.[14] The attached $–SO_3H$ groups impart additional dopant property to β–NSA. The addition of water soluble oxidant i.e. APS initiates the polymerization which only took place at the micelle–water interface.[15] As the polymerization progress, the micelles containing FA particles would become bigger spheres by accretion[16] or rods–fibers by elongation,[17] depending upon the local reaction surroundings. The oxidation of aniline leads to formation of anilinium radical cations which subsequently combine with another unit to form neutral dimer. Further oxidation of this dimer leads to the formation of a trimer, tetramer and finally the formation of polymer composites. The above scheme suggests that PANI and FA assemble polymer composite in tube like structure through a self assembly process. If this were the case, the FA particles would be detected in the wall of the polymer tubes. Schematic representation of incorporation of FA into polyaniline matrix is shown in scheme 1. The presence of flyash particles in polymer matrix is confirmed by the X-ray diffraction patterns of the composites.

A. Conduction mechanism

The room temperature conductivity of composites (Table I) decreases with increase in FA–Aniline weight ratio i.e. from 21.49 Scm^{-1} (PF10) to 2.37 Scm^{-1} (PF13). This can be ascribed to the transport obstruction due to charge carrier scattering, offered by insulating FA phase. The temperature dependence of conductivity has also been studied in the temperature range of 70 to 285 K. Figure 1(a) shows that conductivity increases with temperature like conventional semiconductors. Therefore, we have tried to find suitable models that are available for explaining the transport behavior of disordered semiconductors. The responses of the samples have been analyzed under both Arrhenius[18] as well as Variable range hopping (VRH)[19,20] transport regimes. The Arrhenius–model correlates the conductivity with temperature (T) and activation energy (E_A) as: $\sigma = \sigma_0 \exp(-E_A/K_BT)$ whereas in the VRH model, temperature dependent conductivity (σ_{dc}) can be expressed as $\sigma = \sigma_0 \exp[(-T_0/T)^{\gamma}]$, where To is the Mott characteristic temperature and is a measure of the hopping barrier. The prefactor 'σ_o' represents conductivity at infinite temperature. Their values are determined by density of

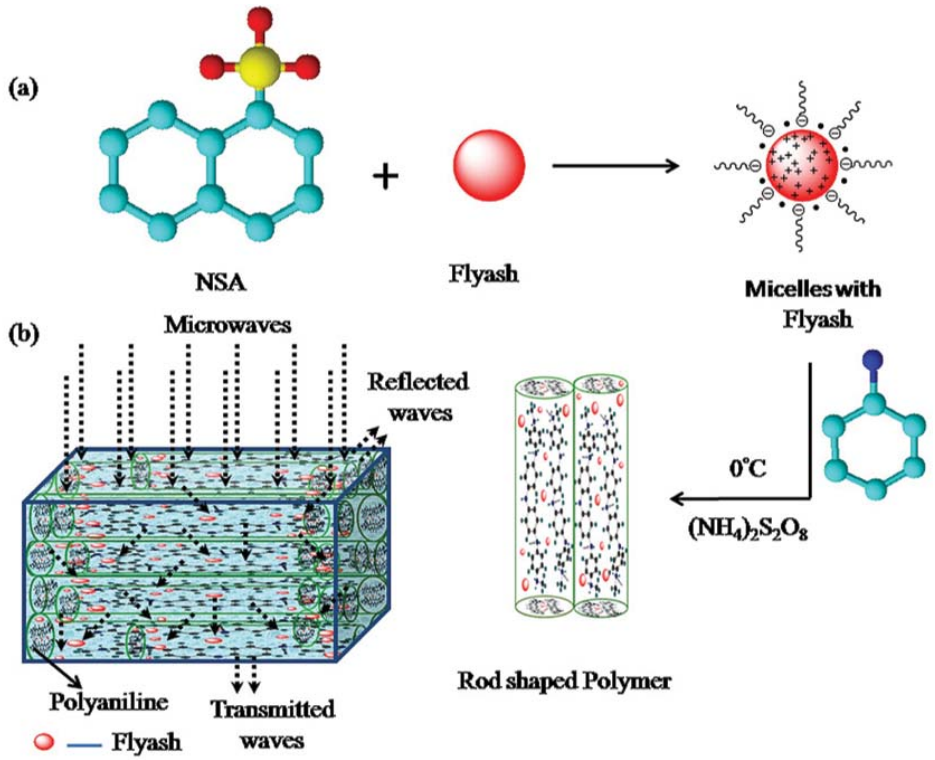

SCHEME 1. Schematic representation of (a) Polymerization of aniline containing the FA particles using APS as oxidant in the presence of β–NSA leads to formation of PANI tubes and (b) the interaction of the microwave with the polymer composite resulting in attenuation due to scattering with the FA particles.

localized states at Fermi energy [$N(E_F)$] and localization length (α^{-1}). The exponent (γ) can be related to dimensionality (d) of the transport system as: $\gamma = 1/(d+1)$ where d equals to 1, 2, and 3 for the 1D, 2D and 3D transport systems respectively. Figure 1(b) shows that the plots of ln σ_{dc} versus T^{-1} have been linear only in high temperature region and fits poorly at low temperatures, indicating the inapplicability of Arrhenius model. However, when plotted under Mott's regime all samples show linearity with various fit parameters. It has been observed that for pure PANI (PF10) sample, plots of ln σ_{dc} vs. $T^{-1/4}$ shows poor fitting as compared to ln σ_{dc} vs $T^{-1/2}$ indicating applicability of 1D–VRH. However, in case of PANI–FA composites, linearity fit factors for ln σ_{dc} vs. $T^{-1/4}$ plots have been better than that for ln σ_{dc} vs $T^{-1/2}$ plots. Therefore, 3D–VRH seems to be the appropriate transport mechanism. The choice of proper transport system has also been ascertained by measuring the slopes (which represents exponent 'γ') of reduced activation energy[21] versus temperature plots on logarithmic scale.[13] This change in transport mechanism (by incorporation of FA) from 1D to 3D VRH may be related to the morphology of the composites. The various factors like reduction in tube length and increase in tube diameter (SEM images), incorporation of insulating FA flakes between PANI chains leading to increased disorder (X–ray diffractograms), and decrease in doping level and effective conjugation (UV–Visible results), may hinder the preferential charge transport along tubular direction, making 3D hopping more probable than 1D transport. The Mott parameters ('T_o' and 'σ_o') for 3D–VRH are given by[22]

$$T_0 = \lambda\alpha^3/k_B N_{3D}(E_F) \tag{1}$$

$$\sigma_0 = e^2(R_{hop})^2 \nu_{ph} N_{3D}(E_F) \tag{2}$$

where, ν_{ph} is phonon frequency ($\sim 10^{13}$ Hz), λ is dimensionless constant ($\sim$18.1), α^{-1} is the localization length and $N(E_F)$ is the density of states at the Fermi energy. The hopping distance (R_{hop})

TABLE I. DC Conductivity, activation energy and Mott's parameters of PANI–FA composites.

Sample	σ (S/cm)	σ_0 S/cm)	T_0 (K)	$N(E_F)$ (eV^{-1} cm^{-3})	R_{hop} (A^0)	W_{hop} (eV)
PF10	21.49	138.34	970.32	7.97 x10^8	220.50	0.018
PF11	17.06	269.55	15954.88	4.89x10^{23}	307.31	0.017
PF12	7.04	248.99	44002.13	1.77 x10^{22}	704.77	0.038
PF13	2.37	138.19	74587.44	1.04x10^{23}	452	0.025

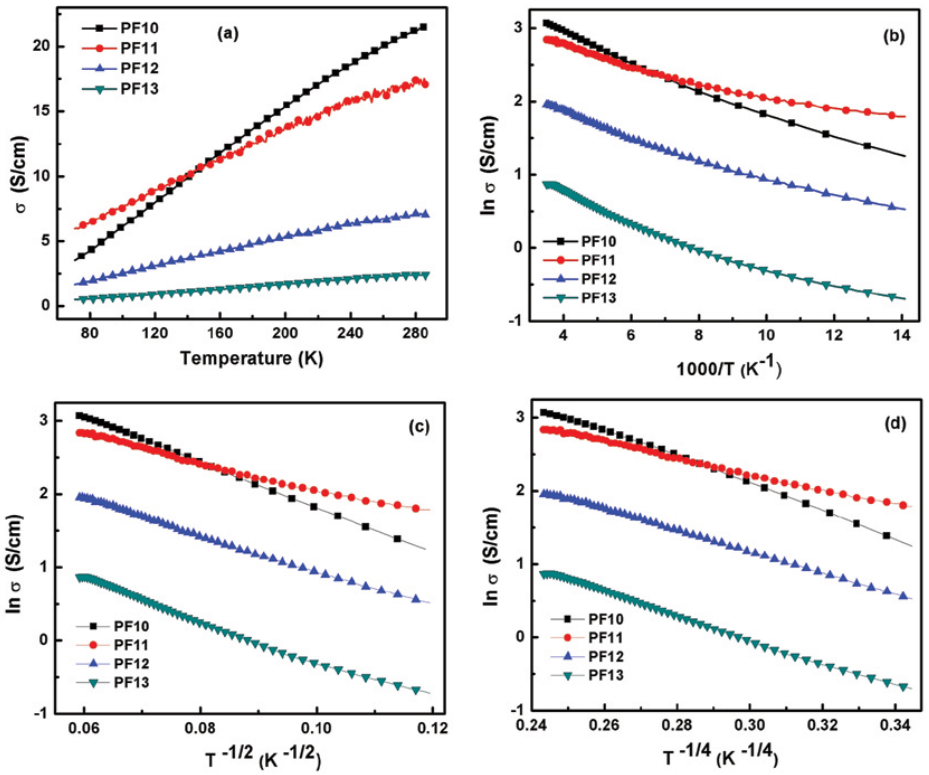

FIG. 1. (a) Variation of conductivity (σ) as a function of temperature in the temperature range 285–70K for PANI–FA composites. (b) lnσ versus 1000/T (c) lnσ verses $T^{-1/2}$ (d) lnσ verses $T^{-1/4}$.

and hopping energy (W_{hop}) are given by following expressions:[23]

$$R_{hop} = [9/8\alpha\pi k_B T N_{3D}(E_F)]^{\frac{1}{4}} \tag{3}$$

$$W_{hop} = [3/4\pi(R_{hop})^3 N_{3D}(E_F)] \tag{4}$$

Therefore, $N_{3D}(E_F)$, R_{hop} and W_{hop} can be calculated from the observed values of T_o (using equation (1)–(4)) and assuming α^{-1} to be ~3Å i.e. width of aniline monomer unit. The calculated Mott parameters are presented in table I. The data shows that T_o increases on increasing the amount of FA in the composite. This is again related to the insulating nature of FA phase and consequent obstruction of charge flow. The calculated $N(E_F)$ decreases in going from PF10 to PF13 which may be related to the decrease in concentration of charge carriers. The increase in hopping distance and hopping energy may be related to increase in system disorder.

B. Electromagnetic shielding & dielectric studies

The EMI shielding effectiveness (SE) of a material is defined as the ratio of transmitted power to incident power and given by $SE_T\,(dB) = 10\log\{P_T/P_I\} = 10\log\{E_T/E_I\} = 10\log\{H_T/H_I\}$ where P_I (E_I or H_I) and P_T (E_T or H_T) are the power (electric or magnetic field) of incident and transmitted EM waves respectively. The total shielding effectiveness can further be divided into three components $SE_T = SE_A + SE_R + SE_M$ where SE_R, SE_A and SE_M are shielding effectiveness due to reflection, absorption and multiple reflections respectively. The scattering parameters S_{11} (or S_{22}) and S_{21} (or S_{12}) of a two port network analyzer can be related with reflectance and transmittance as, $T = |E_T/E_I|^2 = |S_{21}|^2 = |S_{12}|^2$, $R = |E_R/E_I|^2 = |S_{11}|^2 = |S_{22}|^2$. The absorbance (A) can be written as, $A = (1 - R - T)$, Here, it should be noted that the absorption coefficient is given with respect to the power of the incident EM wave. When SE_A is ≥ 10 dB, SE_M is negligible.[23] Therefore, SE_M vanishes and SE_T can be conveniently expressed as: $SE_T = SE_R + SE_A$. The relative intensity of the effectively incident EM wave inside the materials after first reflection is based on the quantity (1-R). Therefore, the effective absorbance (A_{eff}) can be described as $A_{eff} = (1 - R - T)/(1 - R)$ with respect to the power of the effectively incident EM wave inside the shielding material. Therefore, it is convenient to express the reflection and effective absorption losses in the form of -10log (1-R) and -10log (1-A_{eff}) respectively[24] which give SE_R and SE_A as $SE_R = -10\log(1 - R)$ and $SE_A = -10\log(1 - A_{eff}) = -10\log(T/1 - R)$. For a material, the skin depth (δ) is the distance up to which the intensity of the electromagnetic wave decreases to 1/e of its original strength. The δ is related to angular frequency, relative permeability and total conductivity ($\sigma_T = \sigma_{dc} + \sigma_{ac}$) i.e. According to electromagnetic theory, for electrically thick samples (t>δ), frequency (ω) dependence of far field losses can be expressed in the terms of total conductivity (σ_T), real permeability (μ'), skin depth (δ) and thickness (t) of the shield material as:[24]

$$SE_R(dB) = 10\log\left\{\frac{(1-R)}{16\omega\varepsilon_0\mu'}\right\} \tag{5}$$

$$SE_A(dB) = 20\frac{t}{\delta}\log e = 8.68\frac{t}{\delta} \tag{6}$$

The σ_{ac} and δ can be related to imaginary permittivity (ε'') and real permeability (μ') as $\sigma_{AC} = \omega\varepsilon_o\varepsilon'' - \sigma_{dc}$ and $\delta = \sqrt{2/\sigma\omega\mu'}$ which gives absorption loss as: $SE_A(dB) = 8.68t\sqrt{\sigma\omega\mu'/2}$. In microwave range, the contribution of SE_A becomes more as compared to the SE_R. This may be attributed to shallow skin depths and high conductivity (σ_{ac}) values at such high frequencies.

Figure 2 shows the shielding behavior of PANI/FA composite in the frequency range 8.2-12.4 GHz (X-band) and Figure 3(a) shows the variation of the SE_A, SE_R and SE_T with frequency in the 12.4–18 GHz range. From the experimental measurement, the shielding effectiveness due to absorption (SE_A) has been found to vary from 17.31 to 27.29 dB with increase in the FA content while the SE_R decreases from 12.94 to 6.82 dB for the same. Thus, the total SE_T achieved for the PANI-FA composite is 32dB (PF13) which is much higher than the pristine PANI. It has been observed that for conducting PANI-FA composite, shielding effectiveness (SE) is mainly dominated by absorption while the shielding effectiveness due to reflection (SE_R) is nominal and contributes very little. To further investigate the reasons behind the observed increase in SE, the electromagnetic attributes (complex permittivity and permeability) have also been evaluated.

These complex parameters i.e. permittivity ($\varepsilon^* = \varepsilon'$- i$\varepsilon''$) and permeability ($\mu^* = \mu'$- i$\mu''$) of PANI-FA composites, have been calculated from experimental scattering parameters (S_{11} & S_{21}) using theoretical calculations given in Nicholson–Ross and Weir algorithms[25] The real part or dielectric constant (ε') is mainly associated with the amount of polarization occurring in the material and the imaginary part (ε'') is a measure of dissipated energy. The dielectric performance of the material depends on ionic, electronic, orientational and space charge polarization. The contribution to the space charge polarization appears due to the heterogeneity of the material. The presence of insulating FA in the conducting matrix results in the formation of more interfaces and a heterogeneous system due to some space charge accumulating at the interface that contributes toward the higher microwave absorption in the composites. The contribution to the orientational polarization is due to the presence of bound charge (dipoles). In conjugated polymers, two types of charged species are

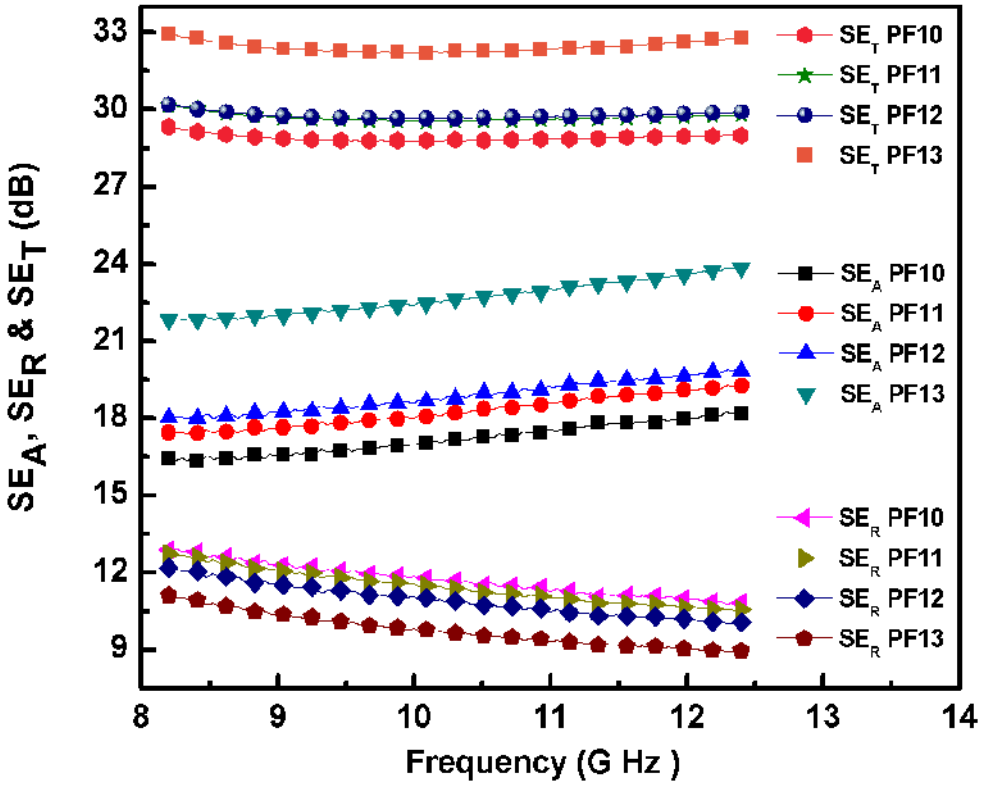

FIG. 2. Dependence of shielding effectiveness (SE_A, SE_R and SE_T) in the frequency range 8.2-12.4 GHz showing the effect of FA concentration on the SE_A valve of PANI–FA composites.

present, one polaron/bipolaron system that is mobile and free to move along the chain, others are bound charges (dipoles) which have only restricted mobility and account for strong polarization in the system.[26] When the frequency of the applied field is increased, the dipoles present in the system cannot reorient themselves fast enough to respond to applied electric field, and as a result, dielectric constant decreases. Due to the difference in the dielectric constant and conductivity of FA and PANI, some charge carriers present in PANI have been trapped, and as a result, space charge is developed on the surface of the FA particles and the polymer. This also leads to the generation of some space charge at the heterogeneous interface leading to field distortion. The contribution of ionic conduction toward the total loss becomes outstanding with decrease in frequency of applied field. With the increase in frequency, the tendency of interfacial polarization is expected to be decreased resulting in a decrease in polarizability and loss factor. Therefore, with the increase in frequency, ε' and ε'' decreases. From Figure 3(b) and 3(c), it is observed that in pristine β–NSA doped PANI (PF10) the dielectric constant (ε') decreases from 70 to 30 with increase of frequency, while on addition of FA in the polymer matrix (PF13), ε' decreases from 43 to 24 with increase of FA content. The dielectric loss (ε'') PANI–FA composite is due to the tubular PANI phase, interfacial polarization between PANI and FA phase. Further, the dielectric losses by SiO_2, $3Al_2O_3.2SiO_2$ and Fe_2O_3 constituents of FA and multiple scattering plays a crucial role in the enhancement of microwave absorption. The increase in FA leads to reduction of skin depth and increase in ac conductivity along with improvement of input impedance. This not only enhances the amount of electromagnetic radiation penetrating inside the shield but also increases the effective absorption capability.

To relate σ_{ac} with the shielding parameter of the material, SE_A is plotted against $(\sigma_{ac})^{1/2}$ (Fig 4(b)). Fig 4(a) shows the variation of σ_{ac} with the increase in frequency for sample PF11, calculated from the dielectric measurements ($\sigma_{ac}=\omega\varepsilon_o\varepsilon''-\sigma_{dc}$). The skin depth of the samples has been calculated using the relation, $\delta = \sqrt{2/\omega\mu\sigma_{ac}}$ and its variation with frequency is shown in

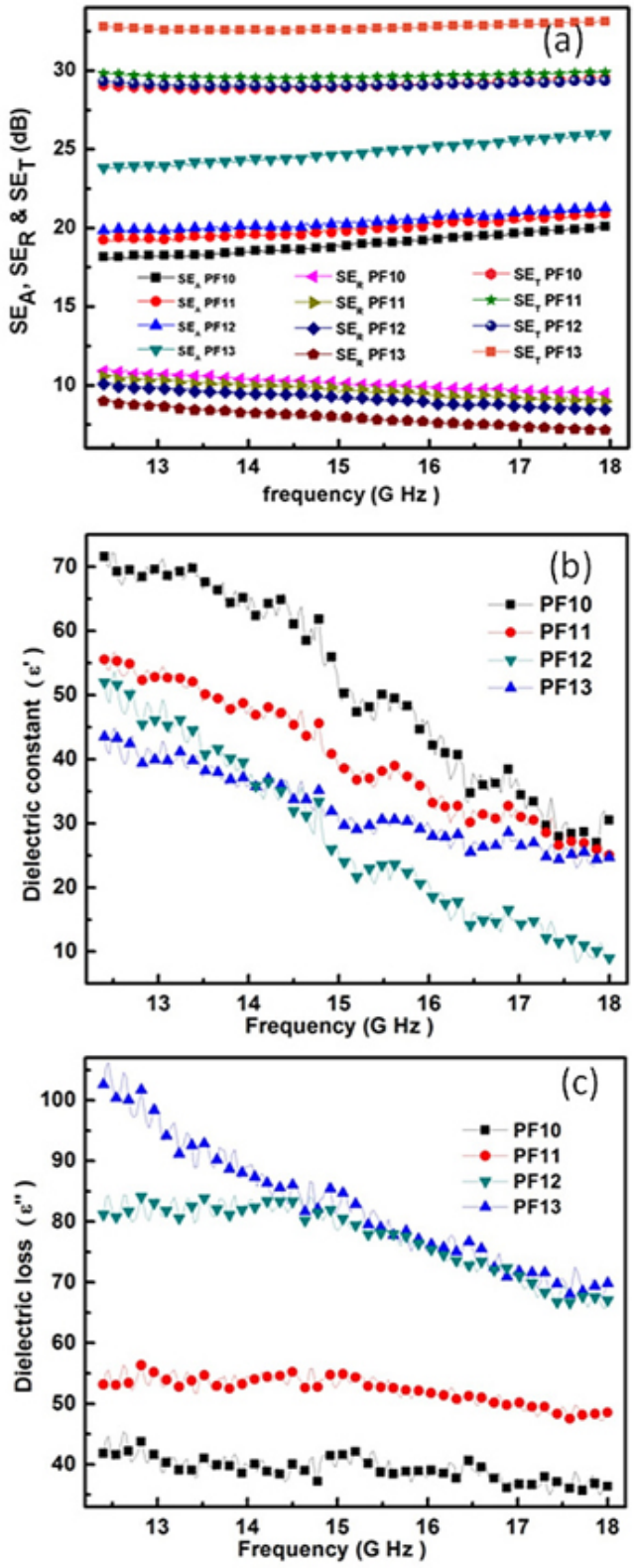

FIG. 3. (a) Dependence of shielding effectiveness (SE_A, SE_R and SE_T) in the frequency range 12.4 – 18 GHz showing the effect of FA concentration on the SE_A valve of PANI–FA composites. Behavior of (b) dielectric constant (ε') and (c) dielectric loss (ε'') of PANI– FA composites as a function of frequency.

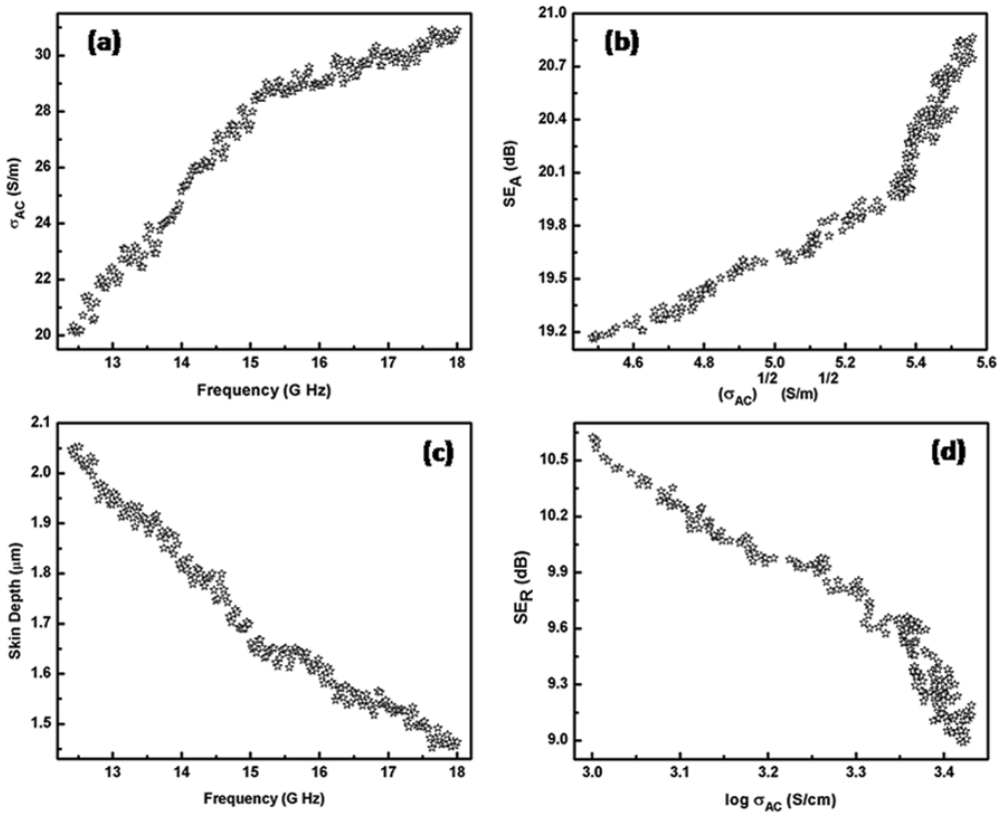

FIG. 4. Variation of ac conductivity (σ_{AC}) as a function of frequency at room temperature (a), Dependence of SE_A as a function of $(\sigma_{AC})^{1/2}$ (b) Change in skin depth (δ) with the increase in frequency (c), and (d) shows the dependence of SE_R as a function of logσ_{AC} for same sample PF11.

Fig 4(c). From the plot it was observed that skin depth decreases with frequency, which demonstrates that mainly surface conduction exists at higher frequencies. The dependence of skin depth on the conductivity and magnetic permeability reveals that, for highly conducting and magnetic material, the skin depth is very small. From equation (6) better SE_A can be achieved from the moderate conducting materials. The dependence of SE_R as a function of log σ_{ac} is shown in figure 4(d). Therefore moderate value of conductivity (σ_{ac}) is required for materials having less shielding effectiveness due to reflection.

C. SEM & EDS analysis

Figure 5 shows the scanning electron micrograph (SEM) and energy dispersive x–ray pattern (EDS) of PANI-FA composite.

SEM image of PANI-FA composites synthesized in presence of β–NSA reveal an interesting morphology featuring formation of tube like structure (Figure 5(a)). Densely packed tubes having a range of diameter and length of $\sim$ 0.5 to 2 μm and up to 15 μm respectively have been observed which is also confirmed by particle size analyzer.[13] SEM micrograph of PANI-FA composites reveals that FA particles are entrapped within the polyaniline matrix (Figure 5(b)). It reduces the length of tubes and gives rise to rough surface. Length and smoothness of PANI/FA tubes is decreased with higher wt% loading of FA particles. Energy dispersive x–ray spectroscopy pattern (EDS) of PF13 (Figure 5(c)) shows the approximate percentage of the constituents of FA like SiO_2, Al_2O_3, Fe_2O_3, CaO present in the composite. The peak of sulfur is due to dopant β–NSA

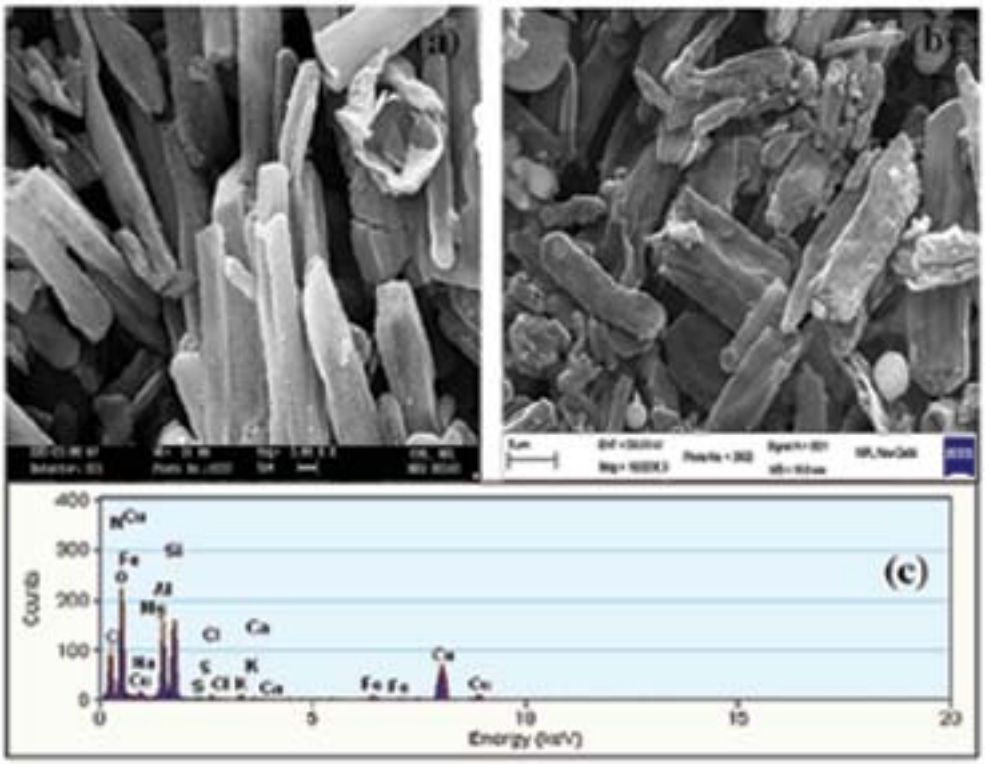

FIG. 5. SEM images of PANI–FA composites (a) PF10 and (b) PF13, showing the formation of tube like structure with FA particles inside the tube and (c) energy dispersive x–ray spectroscopy pattern (EDS) of PF13 showing the approximate percentage of the elements present in the polymer composites.

IV. CONCLUSION

In conclusion, PANI–FA composite has been successfully synthesized using micro emulsion method, which results in core–shell morphology. The formation of tube like structures containing FA particles embedded in between the polymer chains, enhances the interfacial polarization and the effective anisotropy energy of composite, which contributes to more scattering and leads to the high shielding effectiveness ($SE_T \sim 32dB$) as compared to conventional materials. Addition of FA (dielectric filler) in the conducting matrix gave a new kind of composite materials having better microwave absorption properties ($SE_A \sim 25dB$) which strongly depends on volume fraction of FA in PANI matrix. Therefore the high value of EMI SE is dominated by absorption rather than reflection. The charge transport of these composites can be explained in terms of Mott's 3D–VRH model. As a result, polymer composite with dielectric core are also promising as new types of microwave absorption materials with usability in radio frequency range maintaining strong absorption. The presence of conducting shell encapsulating the dielectric filler is helpful for proper impedance matching, which is necessary for enhancing the absorption of the electromagnetic wave.

ACKNOWLEDGMENT

The authors wish to thank Prof. R. C. Budhani, Director, NPL, for his keen interest in the work. The authors thank Kuldeep Singh, Anil Ohlan and Er. Parveen Saini of NPL for their valuable comments and helping in understanding conduction mechanism and suggestions. The authors also thank Dr. Rashmi and K. N. Sood for recording XRD pattern and SEM micrograph.

[1] Fehse K, Schwartz G, Walzer K, Leo K. Combination of a polyaniline anode and doped charge transport layers for high–efficiency organic light emitting diodes. J. Appl. Phys. **101**, 124509 (2007).
[2] Al–Ibrahim M, Ambacher O, Sensfuss S, Gobsch G. Effects of solvent and annealing on the improved performance of solar cells based on poly(3–hexylthiophene): Fullerene. Appl. Phys. Lett **86**, 201120 (2005).
[3] Soto-Oviedo M A, Araujo O A, Faez R, Rezende M C, Paoli M A D. Antistatic coating and electromagnetic shielding properties of a hybrid material based on poly aniline/organoclay nanocomposite and EPDM rubber. Synth. Met. **156**, 1249 (2006).
[4] Ohlan A, Singh K, Chandra A, Dhawan S K. Microwave absorption properties of conducting polymer composite with barium ferrite nanoparticles in 12.4–18 GHz. Appl. Phys. Lett. **93**, 053114 (2008).
[5] Abbas S M, Chatterjee R, Dixit A K, Kumar A V R, Goel T C. Electromagnetic and microwave absorption properties of (Co^{2+}–Si^{4+}) substituted barium hexaferrites and its polymer composite. J. Appl. Phys. **101**, 074105 (2007).
[6] Huang Y, Ma N, Li Y, Du F, Li F, He X, Lin X, Gao H, Chen Y. A plasma enhanced chemical vapor deposition process to achieve branched carbon nanotubes. Carbon **46**, 1614 (2007).
[7] Zhang L, Wan M, Polyaniline/TiO2 Composite Nanotubes. J. Phys. Chem. B **107**, 6748-6753 (2003).
[8] Narayan H, Alemu H, Iwuoha E. Synthesis, characterization and conductivity measurements of polyaniline and polyaniline/fly-ash composites. Phys. stat. sol. (a). **203**, No. 15, 3665–3672 (2006).
[9] Raghavendra S C, Khasim S, Revanasiddappa M, Prasad M, Kulkarni A B. Synthesis, characterization and low frequency a.c. conduction of polyaniline/flyash composites. Bull. Mater. Sci. **26**, 733 (2003).
[10] Dhawan S K, Singh N, Rodrigues D. Electromagnetic shielding behavior of conducting polyaniline composites. Sci. Technol. Adv. Mater. **4**, 105–113(2003).
[11] Jaturapitakkul C, Kiattikomol K, Sata V, Leekeeratikul T. Use of ground coarse fly ash as a replacement of condensed silica fume in producing high-strength concrete. Cem. Concr. Res. **34**, 549–555 (2004).
[12] Michaelson J C, McEvoy A, Interfacial polymerization of aniline. J. Chem. Commun. **79**, (1994).
[13] See Supplementary Material at http://dx.doi.org/10.1063/1.3608052 for Document Nos. 1-5; Document No. 1 for X-ray diffraction studies of Polyaniline and its composite with flyash; Document No. 2 for thermogravimetric analysis of PANI–FA composites with different FA contents at a scan rate 15°C/min in N_2 atmosphere; Document No. 3 for UV-visible spectra of PANI–FA composites with different FA contents. Inset shows the variation of $(\alpha h\nu)^2$ versus $h\nu$ for band gap calculation; Document No. 4 for Activation Energy plot versus temperature Polyaniline-flyash composite; Document No. 5 for Particle size analysis of flyash and flyash-polyaniline composite.
[14] Xia Haibing, SzeOn Chan Hardy, Xiao Changyong, Cheng Daming. Self assembled oriented conducting polyaniline nanotubes. Nanotechnology **15**, 1807–1811 (2004).
[15] Hinrich J, Helfrich W. Fluid and solid fibers made of lipid molecular bilayers. Chem. Rev.**93**, 1565 (1993).
[16] Kim B J, Oh S G, Han M G, Im S S. Preparation of Polyaniline nanoparticles in micellar Solutions as Polymerization Medium. Langmuir **16**, 5841-5845 (2000).
[17] Harada M, Adachi M. Surfactant Mediated Fabrication of Silica Nanotubes. Adv. Mater. **12**, 839-841 (2000).
[18] Reghu M, Cao Y, Moses D, Heeger A. Counterion-induced processibility of polyaniline:Transport at the metal-insulator boundary. J. Phys. Rev. B. **47**, 1758-64 (1993)
[19] Mott N F, Davis E A. *Electronic Processes in Non-Crystalline Materials*, 1st ed.; Clarendon Press: Oxford (1971).
[20] Mott N F, *Metal–Insulator Transition*, 2nd edition, Taylor & Francis. New York, (1990).
[21] Li J, Fang K, Qiu H, Li S, Mao W. Micromorphology and electrical property of the HCl-doped and DBSA-doped polyanilines. Synth Met. **142**, 107 (2004).
[22] Hong Y K, Lee C Y, Jeong C K, Lee D E, Kim K, Joo J. Method and apparatus to measure electromagnetic interference shielding efficiency and its shielding characteristics in broadband frequency ranges. Rev. Sci. Instrum. **74**, 1098 (2003).
[23] Das N C, Das D, Khastgir T K, Chakrraborthy A C. Electromagnetic interference shielding effectiveness of carbon black and carbon fibre filled EVA and NR based composites. Composites A. **31**, 1069 (2000).
[24] Colaneri N F, Shacklette L W. EM1 Shielding Measurements of Conductive Polymer Blends. IEEE Trans. Instrum. Meas. **41**, 29 (1992).
[25] Nicolson A M, Ross G F. Measurement of the Intrinsic Properties of Materials by Time-Domain Techniques IEEE Trans. Instrum Meas. **19**, 377–382 (1970).
[26] Phang S W, Hino T, Abdullah M H, Karamoto N. Applications of polyaniline doubly doped with p-toluene sulphonic acid and dichloroacetic acid as microwave absorbing and shielding materials. Mat. Chem. Phys.; **104**, 327–335 (2007).